Filomat 35:10 (2021), 3241–3266
https://doi.org/10.2298/FIL2110241K

Published by Faculty of Sciences and Mathematics,
University of Niš, Serbia
Available at: http://www.pmf.ni.ac.rs/filomat

Efficient Projective Methods for the Split Feasibility Problem and its Applications to Compressed Sensing and Image Debluring

Suparat Kesornprom[a], Nattawut Pholasa[a], Prasit Cholamjiak[a]

[a]*School of Science, University of Phayao, Phayao 56000, Thailand*

Abstract. In this paper, new projective algorithms using linesearch technique are proposed to solve the split feasibility problem. Weak convergence theorems are established, under suitable conditions, in a real Hilbert space. Some numerical experiments in compressed sensing and image debluring are also provided to show its implementation and efficiency. The main results improve the corresponding results in the literature.

1. Introduction

Let C and Q be nonempty, closed and convex subsets of real Hilbert spaces H_1 and H_2, respectively. In this work, we aim to study the split feasibility problem (SFP) which is to find

$$x^* \in C \text{ such that } Ax^* \in Q \tag{1}$$

where $A : H_1 \to H_2$ is a bounded linear operator. This problem was introduced and studied by Censor and Elfving [9] in Euclidean spaces. Censor et al. in Section 2 of [6] (see also [18]) introduced the prototypical Split Inverse Problem (SIP). In this, there are given two vector spaces X and Y and a linear operator $A : X \to Y$. In addition, two inverse problems are involved. The first one, denoted by IP1, is formulated in the space X and the second one, denoted by IP2, is formulated in the space Y. Given these data, the Split Inverse Problem is formulated as follows: find a point $x^* \in X$ that solves IP1 and such that the point $y^* = Ax^* \in Y$ solves IP2.

In recent years the Nonlinear Split Feasibility Problem (NLSFP) gained a lot of interest, see e.g., [20, 24]. In addition, the non-convex case is also very attractive from the application point of view, see [22].

In what follows, we denote by A^* the adjoint operator of A. Let

$$f(x) = \frac{1}{2}\|(I - P_Q)A(x)\|^2 \tag{2}$$

2020 *Mathematics Subject Classification*. 47H10; 54H25
Keywords. split feasibility problem, projection algorithm, Hilbert space, Weak convergence
Received: 31 October 2019; Revised: 25 May 2020; Revised: 23 October 2020; Revised: 19 December 2020; Accepted: 16 August 2021
Communicated by Marko Petković
Research supported by National Research Council of Thailand (NRCT) and Thailand Science Research and Innovation.
Email addresses: suparat.ke@gmail.com (Suparat Kesornprom), nattawut_math@hotmail.com (Nattawut Pholasa), prasitch2008@yahoo.com (Prasit Cholamjiak)

be an objective function and consider the constrained convex minimization problem:

$$\min_{x\in C} f(x). \tag{3}$$

The split feasibility problem (SFP) is equivalent to constrained convex minimization problem (3).

Since the function f in (2) is differentiable, it is known that $\nabla f = A^*(I - P_Q)A$ and x solves (3) if and only if

$$x = P_C(x - \alpha\nabla f(x)),\ \alpha > 0. \tag{4}$$

This suggests a simple iterative method which is called the projected gradient method for solving (3). It is defined by

$$x_{k+1} = P_C(x_k - \alpha_k \nabla f(x_k)) \tag{5}$$

where $\{\alpha_k\}$ is a positive real sequence.

Korpelevich [17] and Antipin [1] proposed the following extragradient method for solving (3):

$$\begin{aligned} y_k &= P_C(x_k - \alpha_k \nabla f(x_k)), \\ x_{k+1} &= P_C(x_k - \alpha_k \nabla f(y_k)), \end{aligned} \tag{6}$$

where $\{\alpha_k\}$ is a real sequence in $(0, \frac{1}{L})$ and L is a Lipschitz constant of ∇f.

In 2000, Tseng [32] introduced the following modified extragradient method:

$$\begin{aligned} y_k &= P_C(x_k - \alpha_k \nabla f(x_k)), \\ x_{k+1} &= y_k + \alpha_k(\nabla f(x_k) - \nabla f(y_k)), \end{aligned} \tag{7}$$

where $\{\alpha_k\}$ is a real sequence in $(0, \frac{1}{L})$ and L is a Lipschitz constant of ∇f.

The SFP relates to various problems in applied sciences such as signal recovery, image restoration, LASSO problem, linear equations and others. Due to its applications, there have been many algorithms proposed for solving (1). See, for examples, [6, 7, 10, 14–16, 19, 30, 31].

Throughout this paper, we define $F : H_1 \to H_1$ by

$$F(x) = A^*(I - P_Q)A(x). \tag{8}$$

We next recall some well-known algorithms that can be employed for solving (1). Byrne [4, 5] suggested the CQ algorithm which is defined by the following way: $x_1 \in H_1$ and

$$x_{k+1} = P_C(x_k - \alpha_k F(x_k)), \tag{9}$$

where $\alpha_k \in (0, 2/L)$ and L is the spectral radius of A^*A. The notations P_C and P_Q stand for the projections of H_1 onto C and H_2 onto Q, respectively. In practice, the sets C and Q are usually defined by

$$C = \{x \in H_1 : c(x) \le 0\}, \tag{10}$$

where $c : H_1 \to \mathbb{R}$ is a convex and lower semicontinuous function and

$$Q = \{y \in H_2 : q(y) \le 0\}, \tag{11}$$

where $q : H_1 \to \mathbb{R}$ is a convex and lower semicontinuous function.

In 2004, Yang [35] established a relaxed CQ algorithm for solving the SFP. The idea of this method is to replace P_C and P_Q by projections onto half spaces C_k and Q_k. Here the sets C_k and Q_k are defined by

$$C_k = \{x \in H_1 : c(x_k) + \langle \xi_k, x - x_k\rangle \le 0\}, \tag{12}$$

where $\xi_k \in \partial c(x_k)$, and

$$Q_k = \{y \in H_2 : q(Ax_k) + \langle \eta_k, y - Ax_k \rangle \leq 0\}, \tag{13}$$

where $\eta_k \in \partial q(Ax_k)$.

Define $F_k : H_1 \to H_1$ by

$$F_k(x) = A^*(I - P_{Q_k})A(x). \tag{14}$$

Precisely, Yang [35] introduced the following relaxed CQ algorithm.

Algorithm 1. *Let $x_1 \in H_1$ and define*

$$x_{k+1} = P_{C_k}(x_k - \alpha_k F(x_k)) \tag{15}$$

where $\alpha_k \in (0, 2/L)$.

However, the stepsizes in CQ algorithm (9) and relaxed CQ algorithm (15) depend on the spectral radius of A^*A. We note that to compute the spectral radius is difficult in general and this usually results in slow convergence.

Recently, Qu and Xiu [28] modified Yang's relaxed CQ algorithm by using the Armijo-line searches in Euclidean spaces. Later, Gibali et al. [19] proposed the relaxtion CQ algorithm in Hilbert spaces for solving the SFP. It is defined by the following manner:

Algorithm 2. *For any $\sigma > 0$, $\rho \in (0, 1)$ and $\mu \in (0, 1)$. Let $x_1 \in H_1$ and define*

$$y_k = P_{C_k}(x_k - \alpha_k F_k(x_k)) \tag{16}$$

where $\alpha_k = \sigma\rho^{m_k}$ and m_k is the smallest nonnegative integer such that

$$\alpha_k \|F_k(x_k) - F_k(y_k)\| \leq \mu \|x_k - y_k\|. \tag{17}$$

Define

$$x_{k+1} = P_{C_k}(x_k - \alpha_k F_k(y_k)). \tag{18}$$

Gibali et al. [19] proved that the sequence $\{x_n\}$ generated by Algorithm 2 converges weakly to a solution of SFP.

In 2012, Zhao et al. [37] introduced the modified CQ algorithm to solve the SFP as follows:

Algorithm 3. *Let $x_1 \in H_1$, $\sigma_0 > 0$, $\rho \in (0, 1)$, $\mu \in (0, 1)$, $\beta \in (0, 1)$ and let*

$$y_k = P_C(x_k - \alpha_k F(x_k)) \tag{19}$$

where $\alpha_k = \sigma\rho^{m_k}$ and m_k is the smallest nonnegative integer such that

$$\alpha_k \|F(x_k) - F(y_k)\| \leq \mu \|x_k - y_k\|. \tag{20}$$

Define

$$x_{k+1} = P_C(y_k - \alpha_k(F(y_k) - F(x_k))). \tag{21}$$

If

$$\alpha_k \|F(x_{k+1}) - F(x_k)\| \leq \beta \|x_{k+1} - x_k\|, \tag{22}$$

then set $\sigma_k = \sigma_0$, otherwise, set $\sigma_k = \alpha_k$.

Very recently, Dong et al. [12] proposed the modified projection and contraction methods and the relaxation variants to solve the SFP as follows:

Algorithm 4. *For any $\sigma > 0, \rho \in (0,1)$ and $\mu \in (0,1)$, take arbitrarily $x_1 \in H_1$ and let*

$$y_k = P_C(x_k - \alpha_k F(x_k)) \tag{23}$$

where $\alpha_k = \sigma\rho^{m_k}$ and m_k is the smallest nonnegative integer such that

$$\alpha_k \|F(x_k) - F(y_k)\| \leq \mu \|x_k - y_k\|. \tag{24}$$

Define

$$x_{k+1} = x_k - \gamma\delta_k d(x_k, y_k) \tag{25}$$

where $\gamma \in (0,2)$

$$d(x_k, y_k) = (x_k - y_k) - \alpha_k(F(x_k) - F(y_k)) \tag{26}$$

and

$$\delta_k = \frac{\langle x_k - y_k, d(x_k, y_k)\rangle + \alpha_k \|(I - P_Q)A(y_k)\|^2}{\|d(x_k, y_k)\|^2}. \tag{27}$$

They also provided some numerical experiments that show the efficiency of the proposed algorithm.

In this paper, inspired by the previous works, we propose a modification of CQ algorithm and relaxed CQ algorithm to solve the split feasibility problem. We then prove the weak convergence of this algorithm in real Hilbert spaces. Our result mainly improves the results of Dong et al. [12] and others. Some preliminary experiments are also given in compressed sensing and image debluring to show its implementation and efficiency.

2. Preliminaries and lemmas

In this section, we give some definitions and lemmas which are used in the main results. Let H be a real Hilbert space and C be a nonempty subset of H.

(1) A mapping $T : C \to C$ is said to be *firmly nonexpansive* if, for all $x, y \in C$,

$$\langle x - y, Tx - Ty\rangle \geq \|Tx - Ty\|^2. \tag{28}$$

(2) A function $f : H \to \mathbb{R}$ is said to be *convex* if

$$f(\lambda x + (1-\lambda)y) \leq \lambda f(x) + (1-\lambda) f(y) \tag{29}$$

for all $\lambda \in (0,1)$ and $x, y \in H$.

(3) F is said to be monotone on C if

$$\langle F(x) - F(y), x - y\rangle \geq 0, \ \forall x, y \in C. \tag{30}$$

(4) F is said to be τ_n-inverse strongly monotone (shortly, τ_n-ism) with $\tau_n > 0$ if

$$\langle F(x) - F(y), x - y\rangle \geq \tau_n \|F(x) - F(y)\|^2, \ \forall x, y \in C. \tag{31}$$

(5) F is said to be Lipschitz continuous on C with constant $\lambda > 0$ if

$$\|F(x) - F(y)\| \leq \lambda \|x - y\|, \ \forall x, y \in C. \tag{32}$$

(6) A mapping $f : C \to C$ is said to be a contraction if there exists a constant $a \in (0,1)$ such that

$$\|f(x) - f(y)\| \leq a\|x - y\|, \ \forall x, y \in C. \tag{33}$$

(7) A differentiable function f is convex if and only if there holds the inequality:

$$f(z) \geq f(x) + \langle \nabla f(x), z - x \rangle \tag{34}$$

for all $z \in H$.

(8) An element $g \in H$ is called a *subgradient* of $f : H \to \mathbb{R}$ at x if

$$f(z) \geq f(x) + \langle g, z - x \rangle \tag{35}$$

for all $z \in H$, which is called the *subdifferentiable inequality*.

(9) A function $f : H \to \mathbb{R}$ is said to be *subdifferentiable* at x if it has at least one subgradient at x.

(10) The set of subgradients of f at the point x is called the *subdifferentiable* of f at x, which is denoted by $\partial f(x)$.

(11) A function f is said to be *subdifferentiable* if it is subdifferentiable at all $x \in H$. If a function f is differentiable and convex, then its gradient and subgradient coincide.

(12) A function $f : H \to \mathbb{R}$ is said to be *weakly lower semi-continuous* (shortly, w-lsc) at x if $x_n \rightharpoonup x$ implies

$$f(x) \leq \liminf_{n\to\infty} f(x_n). \tag{36}$$

We know that the orthogonal projection P_C from H onto a nonempty closed convex subset $C \subset H$ is a typical example of a firmly nonexpansive mapping, which is defined by

$$P_C x := \arg\min_{y \in C} \|x - y\|^2 \tag{37}$$

for all $x \in H$.

Lemma 1. [3] *Let C be a nonempty closed convex subset of a real Hilbert space H. Then, for any $x \in H$, the following assertions hold:*

(1) $\langle x - P_C x, z - P_C x \rangle \leq 0$ *for all* $z \in C$;

(2) $\|P_C x - P_C y\|^2 \leq \langle P_C x - P_C y, x - y \rangle$ *for all* $x, y \in H$;

(3) $\|P_C x - z\|^2 \leq \|x - z\|^2 - \|P_C x - x\|^2$ *for all* $z \in C$.

From Lemma 1, the operator $I - P_C$ is also firmly nonexpansive, where I denotes the identity operator, i.e., for any $x, y \in H$,

$$\langle (I - P_C)x - (I - P_C)y, x - y \rangle \geq \|(I - P_C)x - (I - P_C)y\|^2. \tag{38}$$

Lemma 2. *[21] Let C be a nonempty subset of a real Hilbert space H and $\{x_n\}$ be a sequence in H that satisfies the following properties:*

(1) $\lim_{n\to\infty} \|x_n - x\|$ *exists for each* $x \in C$;

(2) *every sequential weak limit point of* $\{x_n\}$ *is in* C.

Then $\{x_n\}$ *converges weakly to a point in* C.

3. The modified projection and contraction methods

In this section, we introduce a projection algorithm using linesearch and prove the weak convergence. Assume that the SFP (1) is consistent, i.e. its solution set, denoted by S, is nonempty.

Algorithm 5. *Set* $\sigma > 0, \rho \in (0, 1)$ *and* $\mu \in (0, \frac{1}{2})$. *Choose* $x_1 \in H_1$ *and define*

$$y_k = P_C(x_k - \alpha_k F(x_k)) \tag{39}$$

where $\alpha_k = \sigma\rho^{m_k}$ *and* m_k *is the smallest nonnegative integer such that*

$$\alpha_k\|F(x_k) - F(y_k)\| \leq \mu\|x_k - y_k\|. \tag{40}$$

Define

$$x_{k+1} = y_k - \gamma\delta_k d(x_k, y_k) \tag{41}$$

where $\gamma \in (0, 2)$

$$d(x_k, y_k) = (x_k - y_k) - \alpha_k(F(x_k) - F(y_k)) \tag{42}$$

and

$$\delta_k = \frac{\alpha_k\|(I - P_Q)Ay_k\|^2}{\gamma\|d(x_k, y_k)\|^2}. \tag{43}$$

Remark 1. *If* $d(x_k, y_k) = 0$, *then*

$$\langle x_k - y_k - \alpha_k(F(x_k) - F(y_k)), x_k - y_k\rangle = 0. \tag{44}$$

From (44), it follows that

$$\begin{aligned} \|x_k - y_k\|^2 &= \alpha_k\langle F(x_k) - F(y_k), y_k - x_k\rangle \\ &\leq \alpha_k\|F(x_k) - F(y_k)\|\|x_k - y_k\| \\ &\leq \mu\|x_k - y_k\|^2, \end{aligned} \tag{45}$$

which gives

$$x_k = y_k, \ \forall k \geq 0 \tag{46}$$

From definition of y_k, *we see that*

$$x_k = P_C(x_k - \alpha_k F(x_k)) \tag{47}$$

Hence, $x_k = y_k$ *is a solution.*

Lemma 3. *[36] The line rule (40) is well defined. Besides,* $\alpha' \leq \alpha_k \leq \sigma$, *where* $\tau' = \min\{\sigma, \frac{\mu\rho}{L}\}$.

This lemma shows that the linesearch (40) has a finite number of iteration for α_k.

Theorem 1. *The sequence* $\{x_k\}$ *generated by Algorithm 5 weakly converges to a solution in S.*

Proof. Let $z \in S$. Then $z = P_C(z)$ and $Az = P_Q(Az)$. It follows that

$$\begin{aligned} \|x_{k+1} - z\|^2 &= \|y_k - \gamma\delta_k d(x_k, y_k) - z\|^2 \\ &= \|y_k - z\|^2 - 2\gamma\delta_k\langle y_k - z, d(x_k, y_k)\rangle + \gamma^2\delta_k^2\|d(x_k, y_k)\|^2. \end{aligned} \tag{48}$$

By the definitions of y_k and $d(x_k, y_k)$, we get

$$y_k = P_C(y_k - (\alpha_k F(y_k) - d(x_k, y_k))). \tag{49}$$

From Lemma 1 (1), it follows that

$$\langle x - y_k, \alpha_k F(y_k) - d(x_k, y_k)\rangle \geq 0, \forall x \in C. \tag{50}$$

Setting $x = z$ in (56), we have

$$\langle y_k - z, d(x_k, y_k) - \alpha_k F(y_k)\rangle \geq 0 \tag{51}$$

which implies that

$$\langle y_k - z, d(x_k, y_k)\rangle \geq \alpha_k \langle y_k - z, F(y_k)\rangle. \tag{52}$$

Since $F(y_k) = A^*(I - P_Q)Ay_k$ and $Az = P_Q(Az)$, it follows that

$$\begin{aligned}
\alpha_k\langle y_k - z, F(y_k)\rangle &= \alpha_k\langle y_k - z, A^*(I - P_Q)Ay_k\rangle \\
&= \alpha_k\langle Ay_k - Az, (I - P_Q)Ay_k\rangle \\
&= \alpha_k\langle Ay_k - Az, (I - P_Q)Ay_k - (I - P_Q)Az\rangle \\
&\geq \alpha_k\|(I - P_Q)Ay_k\|^2,
\end{aligned} \tag{53}$$

where the last inequality follows by the firm nonexpansiveness of $I - P_Q$. By Lemma 1(3), we have

$$\begin{aligned}
\|y_k - z\|^2 &= \|P_C(x_k - \alpha_k F(x_k)) - z\|^2 \\
&\leq \|x_k - \alpha_k F(x_k) - z\|^2 - \|y_k - x_k + \alpha_k F(x_k)\|^2 \\
&= \|x_k - z\|^2 - 2\alpha_k\langle x_k - z, F(x_k)\rangle + \alpha_k^2\|F(x_k)\|^2 - \|y_k - x_k\|^2 \\
&\quad -2\alpha_k\langle y_k - x_k, F(x_k)\rangle - \alpha_k^2\|F(x_k)\|^2 \\
&= \|x_k - z\|^2 - 2\alpha_k\langle x_k - z, F(x_k)\rangle - \|y_k - x_k\|^2 - 2\alpha_k\langle y_k - x_k, F(x_k)\rangle.
\end{aligned} \tag{54}$$

Since $F(z) = 0$ and $I - P_Q$ is firmly nonexpansive, it also follows that

$$\begin{aligned}
2\alpha_k\langle x_k - z, F(x_k)\rangle &= 2\alpha_k\langle x_k - z, F(x_k) - F(z)\rangle \\
&= 2\alpha_k\langle x_k - z, A^*(I - P_Q)Ax_k - A^*(I - P_Q)Az\rangle \\
&= 2\alpha_k\langle Ax_k - Az, (I - P_Q)Ax_k - (I - P_Q)Az\rangle \\
&\geq 2\alpha_k\|(I - P_Q)Ax_k\|^2.
\end{aligned} \tag{55}$$

On the other hand, using (34), we obtain

$$\begin{aligned}
2\alpha_k\langle y_k - x_k, F(x_k)\rangle &= 2\alpha_k\langle y_k - x_k, F(x_k) - F(y_k) + F(y_k)\rangle \\
&= 2\alpha_k\langle y_k - x_k, F(x_k) - F(y_k)\rangle + 2\alpha_k\langle y_k - x_k, F(y_k)\rangle \\
&\geq -2\alpha_k\|y_k - x_k\|\|F(x_k) - F(y_k)\| \\
&\quad +2\alpha_k\frac{1}{2}(\|(I - P_Q)Ay_k\|^2 - \|(I - P_Q)Ax_k\|^2) \\
&= -2\alpha_k\|y_k - x_k\|\|F(x_k) - F(y_k)\| \\
&\quad +\alpha_k\|(I - P_Q)Ay_k\|^2 - \alpha_k\|(I - P_Q)Ax_k\|^2.
\end{aligned} \tag{56}$$

Combining (54)-(56), we obtain

$$\begin{aligned}
\|y_k - z\|^2 \leq\ & \|x_k - z\|^2 - 2\alpha_k\|(I - P_Q)Ax_k\|^2 - \|y_k - x_k\|^2 + 2\alpha_k\|y_k - x_k\|\|F(x_k) - F(y_k)\| \\
& -\alpha_k\|(I - P_Q)Ay_k\|^2 + \alpha_k\|(I - P_Q)Ax_k\|^2.
\end{aligned} \tag{57}$$

From (40), (48) and Lemma 3, we have

$$\begin{aligned}
\|x_{k+1}-z\|^2 &\leq \|x_k-z\|^2-2\alpha_k\|(I-P_Q)Ax_k\|^2-\|y_k-x_k\|^2+2\mu\|y_k-x_k\|^2\\
&\quad -\alpha_k\|(I-P_Q)Ay_k\|^2+\alpha_k\|(I-P_Q)Ax_k\|^2-2\gamma\delta_k\alpha_k\|(I-P_Q)Ay_k\|^2\\
&\quad +\gamma^2\delta_k^2\|d(x_k.y_k)\|^2\\
&= \|x_k-z\|^2-\alpha_k\|(I-P_Q)Ax_k\|^2-(1-2\mu)\|y_k-x_k\|^2-\alpha_k\|(I-P_Q)Ay_k\|^2\\
&\quad -2\gamma\delta_k\alpha_k\|(I-P_Q)Ay_k\|^2+\gamma^2\delta_k^2\|d(x_k.y_k)\|^2\\
&= \|x_k-z\|^2-\alpha_k\|(I-P_Q)Ax_k\|^2-(1-2\mu)\|y_k-x_k\|^2\\
&\quad -\frac{\alpha_k\|(I-P_Q)Ay_k\|^2\gamma\|d(x_k,y_k)\|^2}{\gamma\|d(x_k,y_k)\|^2}-2\gamma\delta_k\alpha_k\|(I-P_Q)Ay_k\|^2\\
&\quad +\gamma^2\delta_k^2\|d(x_k,y_k)\|^2\\
&= \|x_k-z\|^2-\alpha_k\|(I-P_Q)Ax_k\|^2-(1-2\mu)\|y_k-x_k\|^2-\delta_k\gamma\|d(x_k,y_k)\|^2\\
&\quad -2\gamma\delta_k\alpha_k\|(I-P_Q)Ay_k\|^2+\gamma^2\delta_k\|d(x_k,y_k)\|^2\\
&= \|x_k-z\|^2-\alpha_k\|(I-P_Q)Ax_k\|^2-(1-2\mu)\|y_k-x_k\|^2\\
&\quad -\gamma(1-\gamma)\delta_k\|d(x_k,y_k)\|^2-2\gamma\delta_k\alpha_k\|(I-P_Q)Ay_k\|^2\\
&\leq \|x_k-z\|^2-\frac{\mu\ell}{L}\|(I-P_Q)Ax_k\|^2-(1-2\mu)\|y_k-x_k\|^2\\
&\quad -2\gamma\delta_k\frac{\mu\ell}{L}\|(I-P_Q)Ay_k\|^2\\
&\leq \|x_k-z\|^2-\frac{\mu\ell}{L}\|(I-P_Q)Ax_k\|^2-(1-2\mu)\|y_k-x_k\|^2. \qquad (58)
\end{aligned}$$

This shows that the sequence $\{\|x_k-z\|\}$ is decreasing and thus converges to a point in H_1. Hence $\{x_k\}$ is bounded. From (58), we see that

$$\lim_{k\to\infty}\|y_k-x_k\|=0 \qquad (59)$$

and

$$\lim_{k\to\infty}\|(I-P_Q)Ax_k\|=0. \qquad (60)$$

Since the sequence $\{x_k\}$ is bounded, there is a cluster point x^* of $\{x_k\}$ with a subsequence $\{x_{k_i}\}$ weakly converging to x^*. From (59), it follows that $\{x_{k_i}\}$ also weakly converges to x^*.

Next, we show that x^* is in S. From (60) and the boundedness of $\{x_{k_i}\}$, it implies that $Ax^*\in Q$. From (8) and (60), it is easy to see that $\lim_{i\to\infty}\|F(x_{k_i})\|=0$. By (39) and (59), we also have

$$\begin{aligned}
\|x_{k_i}-P_C(x_{k_i})\| &\leq \|x_{k_i}-y_{k_i}\|+\|y_{k_i}-P_C(x_{k_i})\|\\
&\leq \|x_{k_i}-y_{k_i}\|+\alpha_{k_i}\|F(x_{k_i})\|\\
&\to 0,\ \text{as } i\to\infty, \qquad (61)
\end{aligned}$$

which implies $x^*\in C$. So x^* is in S. Hence, we can conclude that the sequence $\{x_k\}$ weakly converges to a point in S. This completes the proof. □

4. The modified relaxation projection and contraction methods

In this section, we introduce the modified relaxation projection and contraction methods.
To this end, we assume that the sets C and Q satisfy the following conditions:
The set C is given by

$$C=\{x\in H_1: c(x)\leq 0\}, \qquad (62)$$

where $c : H_1 \to \mathbb{R}$ is a convex and lower semicontinuous function and C is a nonempty set. The set Q is given by

$$Q = \{y \in H_2 : q(y) \leq 0\}, \tag{63}$$

where $q : H_2 \to \mathbb{R}$ is a convex and lower semicontinuous function and Q is a nonempty set. Assume that c and q are subdifferentiable on C and Q, respectively, and c and q are bounded on bounded sets. Note that this condition is automatically satisfied in finite dimensional spaces.

For any $x \in H_1$, at least one subgradient $\xi \in \partial c(x)$ can be calculated, where $\partial c(x)$ is defined as follows:

$$\partial c(x) = \{z \in H_1 : c(u) \geq c(x) + \langle u - x, z\rangle, \forall u \in H_1\}. \tag{64}$$

For any $y \in H_2$, at least one subgradient $\eta \in \partial q(y)$ can be calculated, where

$$\partial q(x) = \{w \in H_2 : q(u) \geq q(y) + \langle v - y, w\rangle, \forall v \in H_2\}. \tag{65}$$

Define the sets C_k and Q_k by the following half-spaces:

$$C_k = \{x \in H_1 : c(x_k) + \langle \xi_k, x - x_k\rangle \leq 0\}, \tag{66}$$

where $\xi_k \in \partial c(x_k)$, and

$$Q_k = \{y \in H_2 : q(Ax_k) + \langle \eta_k, y - Ax_k\rangle \leq 0\}, \tag{67}$$

where $\eta_k \in \partial q(Ax_k)$.

By the definition of the subgradient, it is clear that $C \subseteq C_k$ and $Q \subseteq Q_k$. The projections onto C_k and Q_k are easy to compute since C_k and Q_k are two half-spaces.

Algorithm 6. *For any constants $\sigma > 0, \rho \in (0, 1)$ and $\mu \in (0, \frac{1}{2})$, let x_1 be arbitrarily in H_1 and define*

$$y_k = P_{C_k}(x_k - \alpha_k F_k(x_k)) \tag{68}$$

where $\alpha_k = \sigma\rho^{m_k}$ and m_k is the smallest nonnegative integer such that

$$\alpha_k \|F_k(x_k) - F_k(y_k)\| \leq \mu\|x_k - y_k\|. \tag{69}$$

Define

$$x_{k+1} = y_k - \gamma\delta_k d(x_k, y_k) \tag{70}$$

where $\gamma \in (0, 2)$,

$$d(x_k, y_k) = (x_k - y_k) - \alpha_k(F_k(x_k) - F_k(y_k)) \tag{71}$$

and

$$\delta_k = \frac{\alpha_k \|(I - P_{Q_k})Ay_k\|^2}{\gamma\|d(x_k, y_k)\|^2}. \tag{72}$$

Theorem 2. *The sequence $\{x_k\}$ generated by Algorithm 6 weakly converges to a solution in S.*

Proof. Following the lines of the proof of Theorem 1, we can show that

$$\begin{aligned} & \|x_{k+1} - z\|^2 \\ \leq\ & \|x_k - z\|^2 - \frac{\mu\ell}{L}\|(I - P_Q)Ax_k\|^2 - (1 - 2\mu)\|y_k - x_k\|^2 - 2\gamma\delta_k\frac{\mu\ell}{L}\|(I - P_Q)Ay_k\|^2 \\ \leq\ & \|x_k - z\|^2 - \frac{\mu\ell}{L}\|(I - P_Q)Ax_k\|^2 - (1 - 2\mu)\|y_k - x_k\|^2. \end{aligned} \tag{73}$$

Moreover, we also have

$$\lim_{k\to\infty} \|y_k - x_k\| = 0 \tag{74}$$

and

$$\lim_{k\to\infty} \|(I - P_{Q_k})Ax_k\| = 0. \tag{75}$$

Let x^* be a cluster point of $\{x_k\}$ with $\{x_{k_i}\}$ converging to x^*. From (74), it follows that $\{x_{k_i}\}$ also weakly converges to x^*.

Next, we show that x^* is in S. In fact, since $y_{k_i} \in C_{k_i}$, by the definition of C_{k_i}, we have

$$c(x_{k_i}) + \langle \xi_{k_i}, y_{k_i} - x_{k_i}\rangle \leq 0, \tag{76}$$

where $\xi_{k_i} \in \partial c(x_{k_i})$. By the assumption that ξ_{k_i} is bounded and (74), we have

$$\begin{aligned} c(x_{k_i}) &\leq -\langle \xi_{k_i}, y_{k_i} - x_{k_i}\rangle \\ &\leq \|\xi_{k_i}\|\|y_{k_i} - x_{k_i}\| \\ &\to 0 \text{ as } i \to \infty, \end{aligned} \tag{77}$$

which implies $c(x^*) \leq 0$ by the lower semicontinuity of C. Hence $x^* \in C$. Since $P_{Q_{k_i}}(Ax_{k_i}) \in Q_{k_i}$, we also have

$$q(Ax_{k_i}) + \langle \eta_{k_i}, P_{Q_{k_i}}(Ax_{k_i}) - Ax_{k_i}\rangle \leq 0, \tag{78}$$

where $\eta_{k_i} \in \partial q(Ax_{k_i})$. From the boundedness of $\{\eta_{k_i}\}$ and (75), it follows that

$$q(Ax_{k_i}) \leq \|\eta_{k_i}\|\|P_{Q_{k_i}}(Ax_{k_i}) - Ax_{k_i}\| \to 0 \tag{79}$$

as $i \to \infty$. So we obtain $q(Ax^*) \leq 0$, i.e., $Ax^* \in Q$. Thus x^* is in S. By Lemma 2, we conclude that $\{x_k\}$ weakly converges to a point in S. We thus complete the proof. □

5. Application to signal recovery

In this section, we test our algorithm to show the efficiency in compressed sensing in frequency domain.

In signal processing, compressed sensing can be modeled as the following under determinated linear equation system:

$$y = Ax + \varepsilon, \tag{80}$$

where $x \in \mathbb{R}^N$ is a vector with m nonzero components to be recovered, $y \in \mathbb{R}^M$ is the observed or measured data with noisy ε, and $A : \mathbb{R}^N \to \mathbb{R}^M$ ($M < N$) is a bounded linear observation operator. Finding the solutions of (80) can be seen as solving the LASSO problem [33]

$$\min_{x\in\mathbb{R}^N} \frac{1}{2}\|y - Ax\|_2^2 \text{ subject to } \|x\|_1 \leq t, \tag{81}$$

where $t > 0$ is a given constant. In particular, if $C = \{x \in \mathbb{R}^N : \|x\|_1 \leq t\}$ and $Q = \{y\}$, then the LASSO problem can be considered as the SFP.

In this experiment, the sparse vector $x \in \mathbb{R}^N$ is generated by the uniform distribution in the interval $[-2, 2]$ with m nonzero elements. The matrix $A \in \mathbb{R}^{M\times N}$ is generated by the normal distribution with mean zero and variance one. The observation y is generated by white Gaussian noise with signal-to-noise ratio SNR=40. The process is started with $t = m$ and initial point $x_1 =$ is picked randomly.

The restoration accuracy is measured by the mean squared error as follows:

$$E_k = \frac{1}{N}\|x_k - x\|_2^2 < \varepsilon, \tag{82}$$

where x_k is an estimated signal of x and ε is a given error.

We give some numerical results of Algorithms 1, 2, 4 and 6 . Let $\sigma = 3$, $\rho = 0.9$, $\gamma = 1.8$ and $\mu = 0.4$. In this numerical experiment, we use Matlab R2018b to write all codes.

We test four cases as follow:
Case 1: $N = 512$, $M = 256$ and $m = 10$;
Case 2: $N = 1024$, $M = 512$ and $m = 30$;
Case 3: $N = 2048$, $M = 1024$ and $m = 50$;
Case 4: $N = 4096$, $M = 2048$ and $m = 100$.

The numerical results are reported as follows.

Table 1: Computational results to recover the signal

	Methods	$\varepsilon = 10^{-3}$		$\varepsilon = 10^{-4}$	
		Iter	CPU	Iter	CPU
Case 1	Algorithm 1	28	0.3973	84	1.3127
	Algorithm 2	30	0.5643	86	1.4148
	Algorithm 4	27	0.5813	36	0.6383
	Algorithm 6	17	0.3389	29	0.6335
Case 2	Algorithm 1	49	3.7598	95	7.7859
	Algorithm 2	51	7.2222	99	14.9803
	Algorithm 4	32	4.6847	47	8.0774
	Algorithm 6	22	3.6419	34	5.8058
Case 3	Algorithm 1	41	30.0557	94	115.8860
	Algorithm 2	43	36.1808	94	93.0088
	Algorithm 4	30	25.3104	37	37.1473
	Algorithm 6	20	17.0654	29	29.5174
Case 4	Algorithm 1	39	248.8680	71	465.5332
	Algorithm 2	41	147.2881	74	264.2121
	Algorithm 4	32	118.6846	60	215.0726
	Algorithm 6	19	74.8502	34	122.7263

In Table 1, we see that our Algorithm 6 has a less number of iterations and CPU time than Algorithms 1, 2 and 4 do in each cases.

Next, we show the graphs of original signal and recovered signal by Algorithms 1, 2,4 and 6 when $N = 512$, $M = 256$, $m = 10$ and $\varepsilon = 10^{-4}$. The number of iterations and CPU time are reported in the figures.

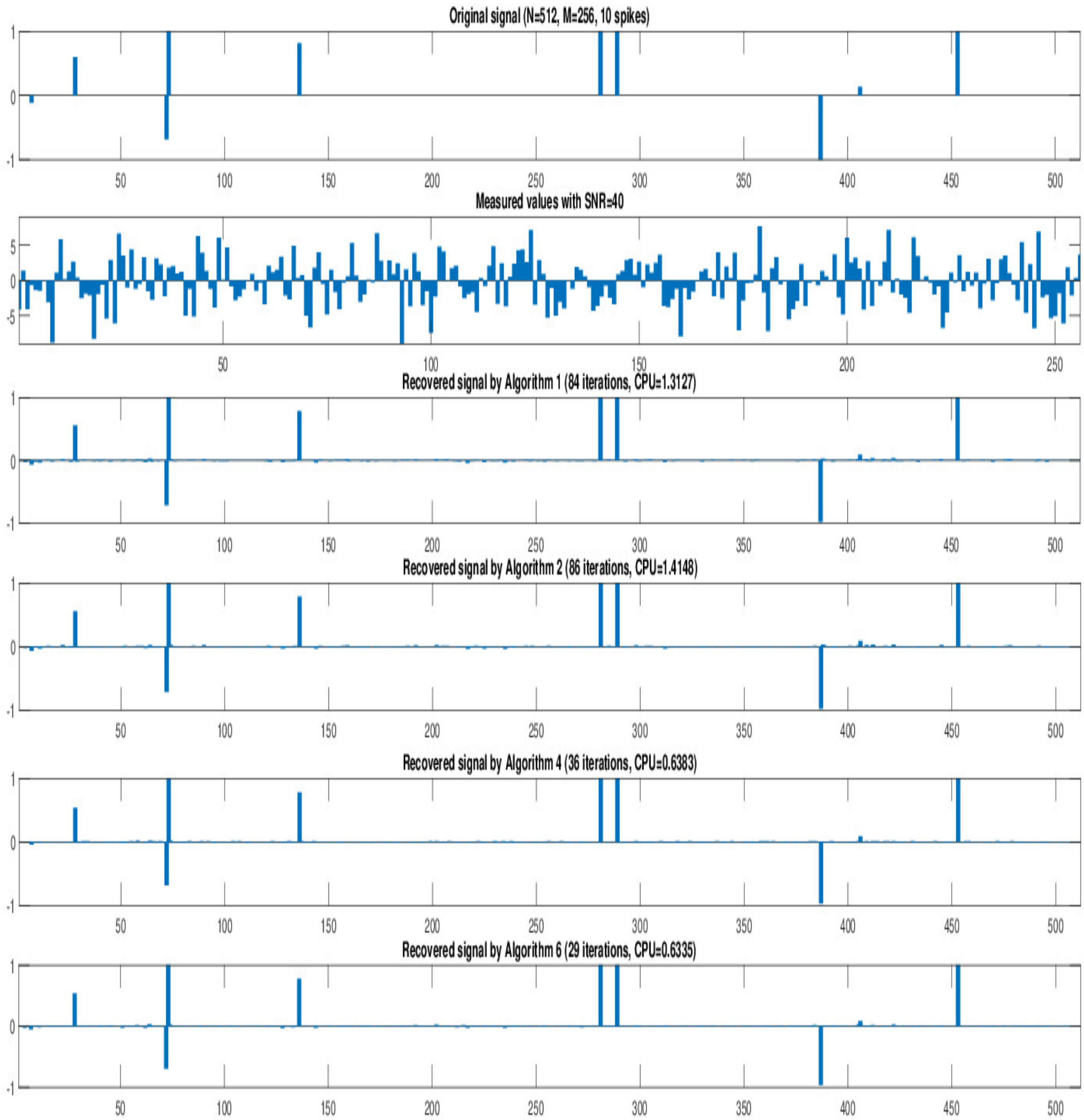

Figure 1: From top to bottom: original signal, observation data, recovered signal by Algorithms 1, 2, 4 and 6 in Case 1, respectively.

We next show the graphs of signal recovery by Algorithms 1, 2, 4 and 6 when $N = 4096$, $M = 2048$, $m = 100$ and $\varepsilon = 10^{-4}$.

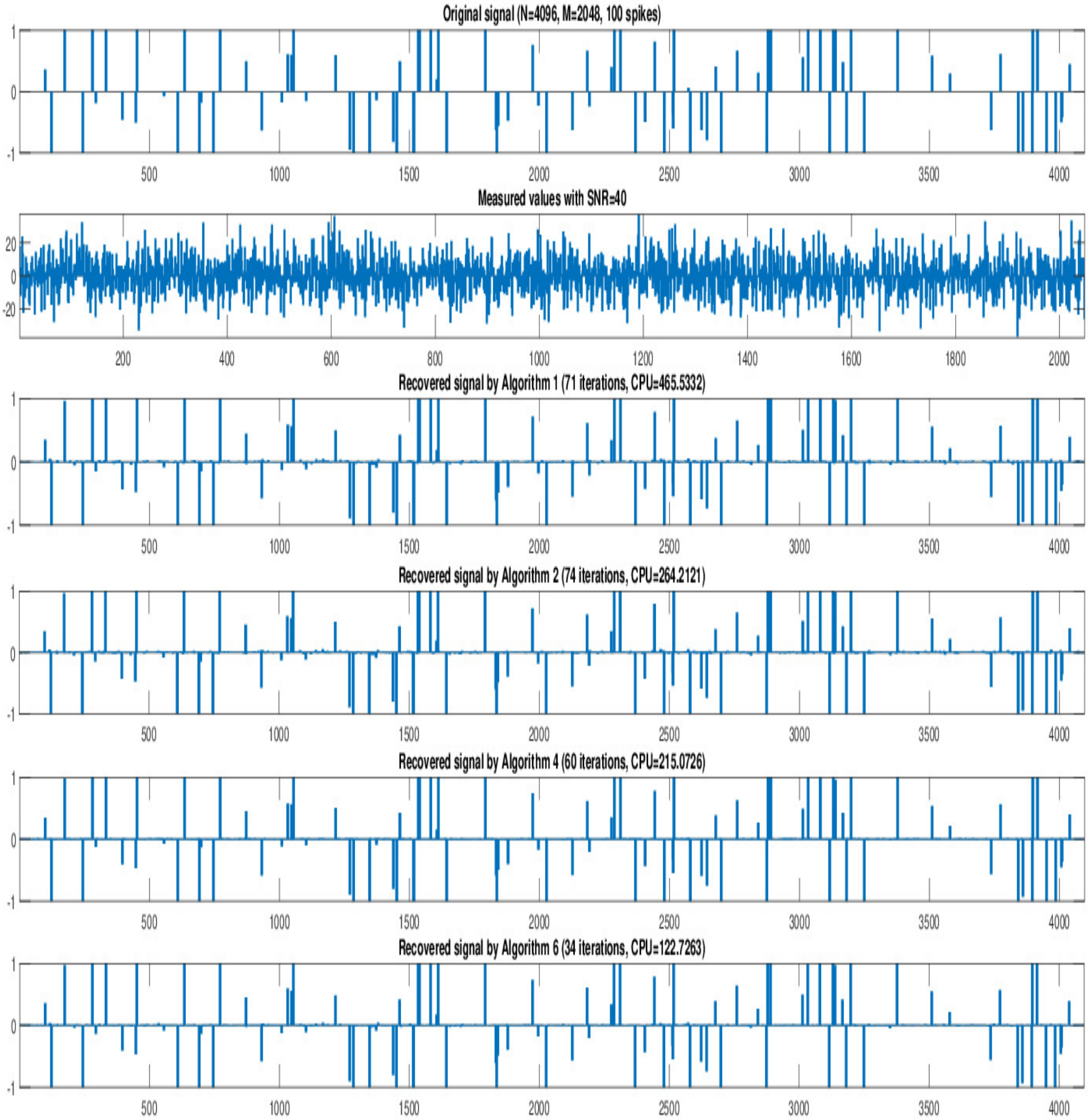

Figure 2: From top to bottom: original signal, observation data, recovered signal by Algorithms 1, 2, 4 and 6 in Case 4, respectively.

We next show the error plotting of Algorithms 1, 2, 4 and 6 in Case 1 and Case 4.

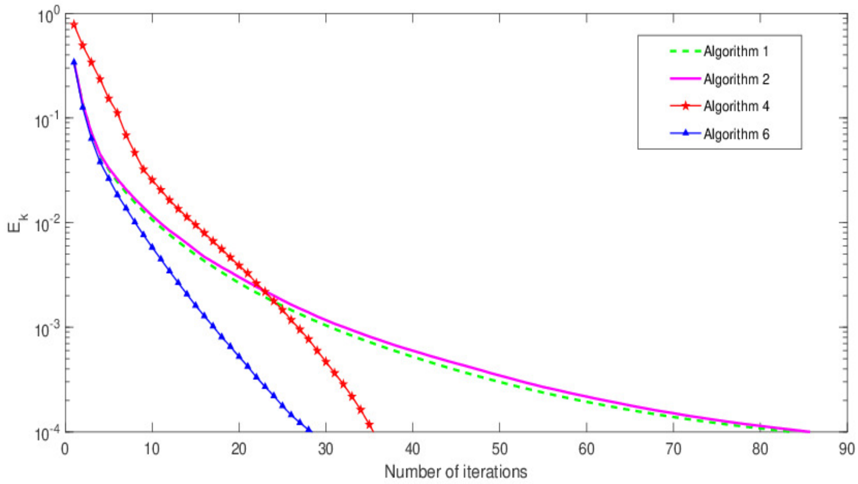

Figure 3: E_k versus number of iterations in Case 1

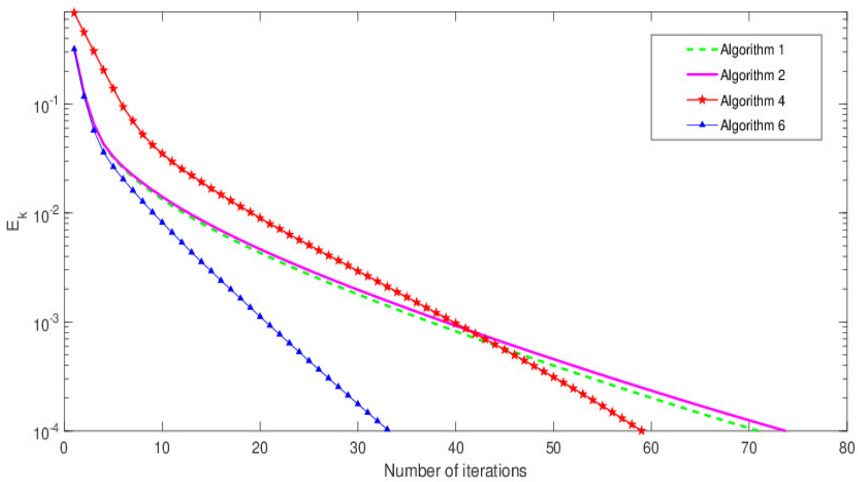

Figure 4: E_k versus number of iterations in Case 4

From Figure 3 and 4, we observe that Algorithms 1, 2, 4 and 6 can be applied to signal recovery problem. Also, we note that Algorithm 6 has a good performance for this problem. It requires a small number of iterations and CPU time in numerical comparison.

6. Application to image restoration

As mentioned earlier that SFP can apply to many real-world problems. In this section, we present an application to image restoration problems using our main result. We provide some comparisons to other algorithms.

For a RGB scale image of M pixels wide by N pixels height, each pixel value is known to range from 0 to 255. Let $D = M \times N$. Then the underlying real Hilbert space is $\mathbb{R}^D$ equipped with the standard Euclidean norm $\|\cdot\|_2$, and let $C = [0, 255]^D$. In order to estimate an approximation of the vector x, which represents the image of the original image scene, we consider the convex minimization model:

$$\min_{x \in C} \|Ax - y\|_2. \tag{83}$$

By choosing $Q = \{y\}$, the problem (83) can be seen as SFP (1). Therefore, we can apply our algorithm to solve image restoration problem.

In this numerical experiment, we use Matlab R2018b to write all codes. To determine the efficiency of algorithms, we need an image quality measure of restored images. We define the Peak Signal-to-Noise Ration (SNR) in decibel (dB) as follows:

$$PSNR = 20 \log_{10} \frac{\|\bar{x}\|_2}{\|x - \bar{x}\|_2}, \tag{84}$$

where $\bar{x}$ is an original image and x is a restored image. It can be observed that the larger PSNR values, the better restored images. To begin, set the initial point x_0 to be $0 \in \mathbb{R}^D$. Set all parameters by $\sigma = 0.1$, $\rho = 0.3$, $\mu = 0.01$ and $\gamma = 0.3$. Each image is degraded by a motion blur with a motion length 15, 30, 45, 60 and an angle 180. Then the numerical results are reported in Tables 2-4.

Table 2: Numerical comparison for Algorithms 3, 4 and 5 of Cat image (size=384 × 512) for each motion length.

			PSNR (dB)		
motion length		Iter	Algorithm 3	Algorithm 4	Algorithm 5
15	Red	500	16.3829	21.8416	28.4803
	15.2780	1500	18.8747	28.0628	31.0661
		2500	20.3751	29.4057	33.3359
	Green	500	16.6123	22.2360	30.0804
	15.5079	1500	19.0836	28.5551	34.9486
		2500	20.5847	29.8299	39.6045
	Blue	500	16.3846	22.1783	30.0731
	15.2867	1500	18.8649	28.2531	32.8363
		2500	20.3506	29.6004	36.1965
30	Red	500	14.3873	18.5316	23.2017
	13.5449	1500	16.2169	23.1547	25.4769
		2500	17.2081	24.3563	27.1030
	Green	500	14.5810	18.8749	24.1111
	13.7345	1500	16.4350	23.4089	27.8878
		2500	17.4299	24.6307	31.2110
	Blue	500	14.3615	18.7789	24.3106
	13.5187	1500	16.1906	23.1145	30.3329
		2500	17.1750	24.2868	34.9843
45	Red	500	13.3905	17.0191	23.3165
	12.6151	1500	15.0767	22.9588	27.3520
		2500	15.9724	24.6974	29.6749
	Green	500	13.5494	17.4840	24.8367
	12.7687	1500	15.2525	23.7401	30.4577
		2500	16.1504	25.6345	33.1714
	Blue	500	13.3591	17.5345	26.0984
	12.5863	1500	15.0876	23.8176	30.0078
		2500	15.9923	25.6284	31.9806
60	Red	500	12.7475	16.6084	20.9304
	11.9738	1500	14.3126	20.6654	23.8163
		2500	15.1075	22.0668	25.6994
	Green	500	12.8991	17.0952	21.6524
	12.1172	1500	14.4934	21.1951	25.7100
		2500	15.3059	22.6414	28.7144
	Blue	500	12.7236	16.9615	22.7128
	11.9738	1500	14.2535	21.1349	27.0384
		2500	15.0523	22.5753	29.3498

Table 3: Numerical comparison for Algorithms 3, 4 and 5 of Flower image (size=436 × 581) for each motion length.

			PSNR (dB)		
motion length		Iter	Algorithm 3	Algorithm 4	Algorithm 5
15	Red 14.5043	500	15.8800	20.9102	28.3568
		1500	18.8107	27.8765	31.1837
		2500	20.3663	29.9398	32.7696
	Green 13.5214	500	14.7885	22.2360	27.7529
		1500	17.6993	28.5551	30.7161
		2500	19.2332	29.8299	34.6631
	Blue 14.5043	500	11.5805	22.1783	25.8711
		1500	14.7687	28.2531	28.7938
		2500	16.3425	29.6004	30.4692
30	Red 11.6408	500	12.6945	17.5511	23.9708
		1500	15.0474	23.6652	27.2366
		2500	16.2712	25.7113	28.5671
	Green 10.8898	500	11.9130	17.2443	23.7777
		1500	14.2947	23.0851	27.8288
		2500	15.5008	25.1728	29.8185
	Blue 7.9578	500	9.0205	14.2360	21.0311
		1500	11.3884	20.4351	23.9368
		2500	12.6548	22.6984	25.3762
45	Red 10.0959	500	11.2232	16.2864	21.6577
		1500	13.8158	20.6374	24.1833
		2500	14.9816	22.4024	26.4041
	Green 9.6107	500	10.6243	15.9176	20.4077
		1500	12.9926	20.1874	25.7436
		2500	14.1141	21.5196	33.2497
	Blue 7.2346	500	8.0913	12.6382	18.4416
		1500	10.1583	18.0640	21.2062
		2500	11.2730	19.7364	23.0863
60	Red 9.1517	500	10.1365	14.8332	21.3515
		1500	12.0693	20.8865	24.0216
		2500	13.1579	22.6918	25.3246
	Green 8.8377	500	9.6996	15.1557	20.2725
		1500	11.6472	20.4646	23.5771
		2500	12.6518	21.9962	25.3317
	Blue 6.8093	500	7.5010	11.6169	17.3878
		1500	9.0997	17.1928	20.1489
		2500	10.0391	19.0494	21.4323

Table 4: Numerical comparison of PSNR values of Temple image (size=581×432) each motion length.

			PSNR (dB)		
motion length		Iter	Algorithm 3	Algorithm 4	Algorithm 5
15	Red 14.2357	500	15.2004	19.0802	27.8120
		1500	17.3632	26.5228	31.0685
		2500	18.7359	28.6759	32.9181
	Green 15.5075	500	16.5184	20.3138	29.3533
		1500	18.7597	27.7870	32.3749
		2500	20.1512	29.7041	34.0459
	Blue 16.7618	500	17.8056	22.4030	30.2959
		1500	20.1113	29.3933	33.5506
		2500	21.5074	31.1807	35.2786
30	Red 12.6488	500	13.4104	16.1524	22.1375
		1500	15.0103	20.9424	24.6278
		2500	15.8666	22.9244	25.7783
	Green 13.7762	500	14.5928	17.4967	23.5112
		1500	16.2930	22.4206	26.0190
		2500	17.2013	24.3866	27.2886
	Blue 14.7636	500	15.6445	18.9835	24.8991
		1500	17.4787	24.4009	27.2539
		2500	18.4356	26.0283	28.4147
45	Red 11.6720	500	12.4420	15.6032	21.9892
		1500	14.0749	21.0037	25.4849
		2500	14.8852	23.2634	27.3369
	Green 12.6974	500	13.5300	16.8465	23.2119
		1500	15.3078	22.4460	25.3298
		2500	16.1652	24.8112	28.5828
		500	14.4353	18.1228	24.5189
	Blue	1500	16.4149	24.0860	28.0582
	13.5125	2500	17.3238	26.1620	29.8786
60	Red 10.9888	500	11.7898	14.5487	19.5199
		1500	13.2249	18.9835	21.7620
		2500	13.9734	20.5929	22.8371
	Green 11.9196	500	12.7634	15.6730	21.0301
		1500	14.3215	20.3644	23.2214
		2500	15.1202	22.0877	24.3413
	Blue 12.6183	500	13.5083	16.7875	22.4595
		1500	15.2758	21.8304	24.6498
		2500	16.1448	23.4691	25.7597

From Tables 2-4, the reports show that PSNR of Algorithm 5 is higher than Algorithm 3 and Algorithm 4 in each motion lengths. From this point of view, we conclude that our proposed Algorithm 5 has a better convergence behavior than Algorithm 3 defined by Zhao et al. [37] and Algorithm 4 defined by Dong et al. [12].

Next, we show the original images for Cat image (size= 384×512), Flower image (size=436×581) and Temple image (size=581×432).

(a) Cat

(b) Flower

(c) Temple

Figure 5: Original images

We next demonstrate the blurred images for each motion length.

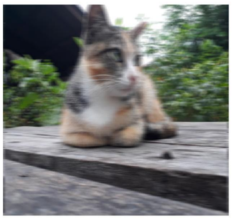

(a) motion length 15

(b) motion length 30

(c) motion length 45

(d) motion length 60

(e) motion length 15

(f) motion length 30

(g) motion length 45

(h) motion length 60

(i) motion length 15

(j) motion length 30

(k) motion length 45

(l) motion length 60

Figure 6: Blurred images

Next, we demonstrate the recovered images by using Algorithms 3, 4 and 5 for the motion length 15 and the number of iterations is 2500.

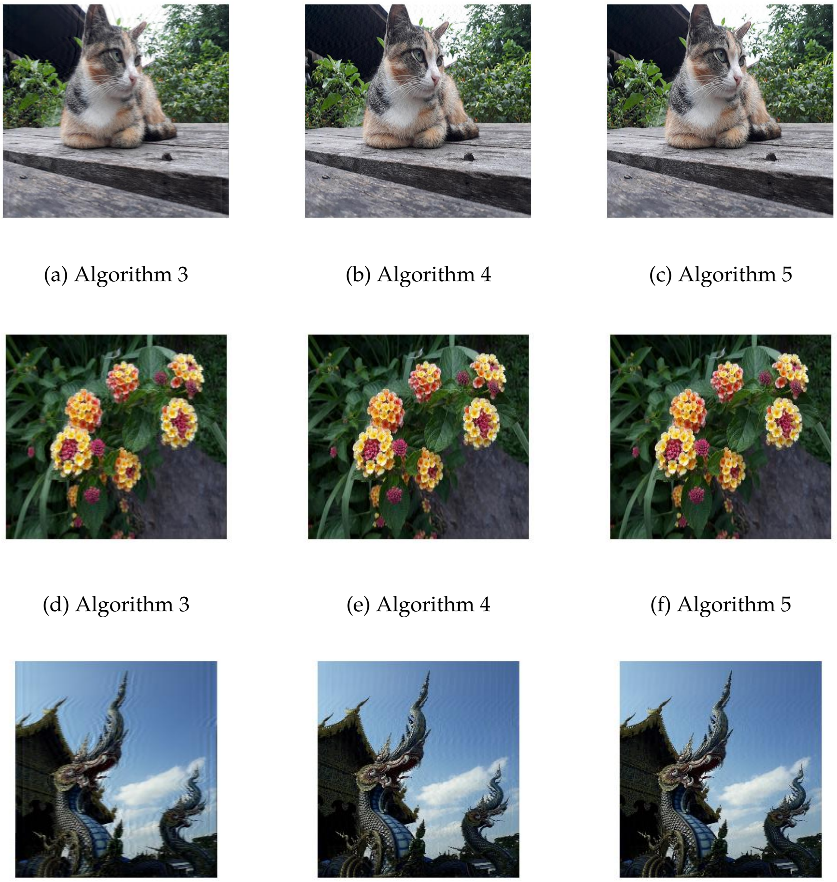

(a) Algorithm 3 (b) Algorithm 4 (c) Algorithm 5

(d) Algorithm 3 (e) Algorithm 4 (f) Algorithm 5

(g) Algorithm 3 (h) Algorithm 4 (i) Algorithm 5

Figure 7: Recovered images with the motion length 15.

We demonstrate the recovered images by using Algorithms 3, 4 and 5 for the motion length 30 and the number of iterations is 2500.

(a) Algorithm 3

(b) Algorithm 4

(c) Algorithm 5

(d) Algorithm 3

(e) Algorithm 4

(f) Algorithm 5

(g) Algorithm 3

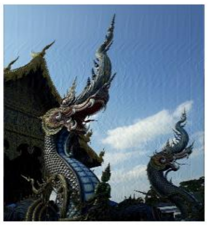

(h) Algorithm 4

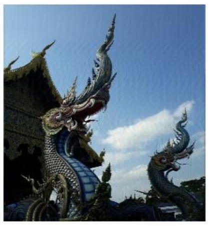

(i) Algorithm 5

Figure 8: Recovered images with the motion length 30.

We demonstrate the recovered images by using Algorithms 3, 4 and 5 for the motion length 45 and the number of iterations is 2500.

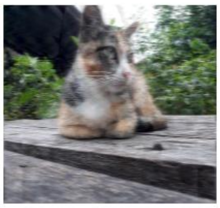

(a) Algorithm 3

(b) Algorithm 4

(c) Algorithm 5

(d) Algorithm 3

(e) Algorithm 4

(f) Algorithm 5

(g) Algorithm 3

(h) Algorithm 4

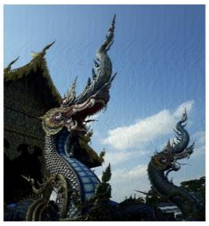

(i) Algorithm 5

Figure 9: Recovered images with the motion length 45.

We demonstrate the recovered images by using Algorithms 3, 4 and 5 for the motion length 60 and the number of iterations is 2500.

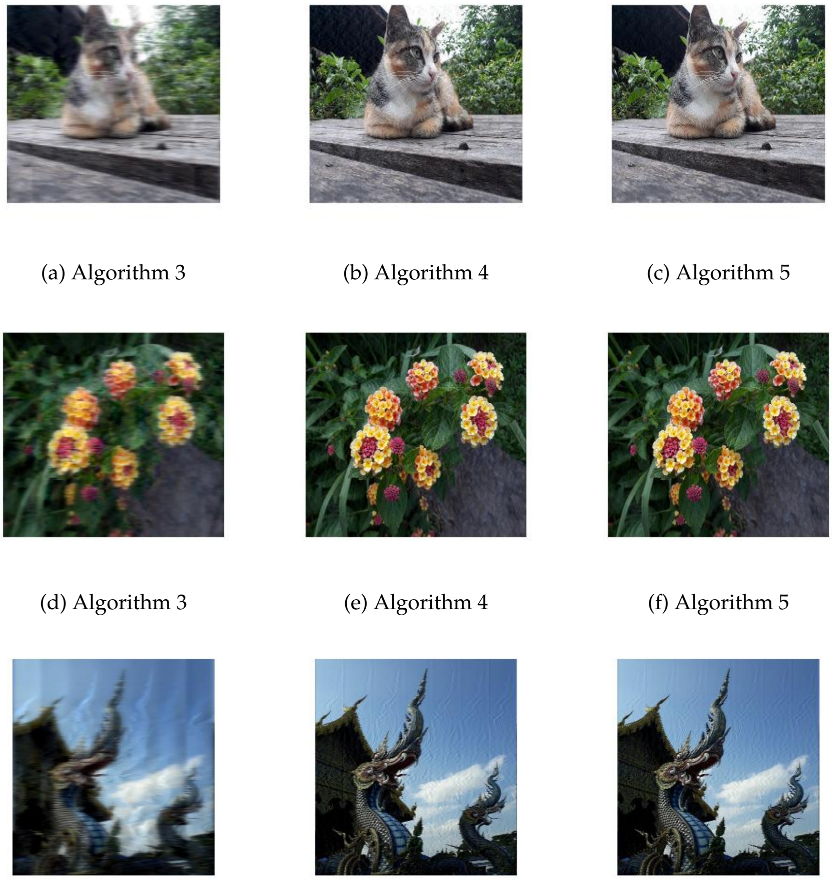

(a) Algorithm 3 (b) Algorithm 4 (c) Algorithm 5

(d) Algorithm 3 (e) Algorithm 4 (f) Algorithm 5

(g) Algorithm 3 (h) Algorithm 4 (i) Algorithm 5

Figure 10: Recovered images with the motion length 60.

We next provide the PSNR plotting of Algorithms 3, 4 and 5.

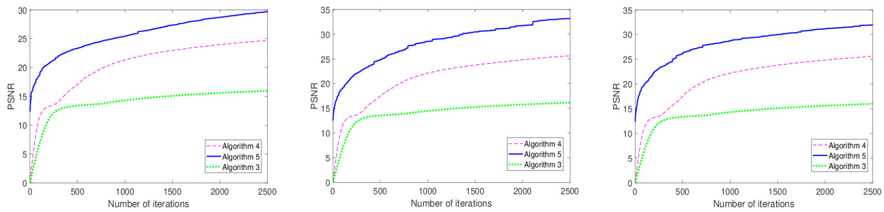

(a) PSNR (Red) (b) PSNR (Green) (c) PSNR (Blue)

Figure 11: Graphs of PSNR for red, green and blue for Algorithms 3, 4 and 5 of Cat image with motion length 45.

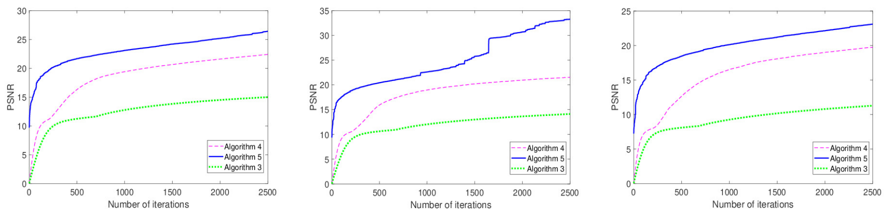

(a) PSNR (Red) (b) PSNR (Green) (c) PSNR (Blue)

Figure 12: Graphs of PSNR for red, green and blue for Algorithms 3, 4 and 5 of Flower image with motion length 45.

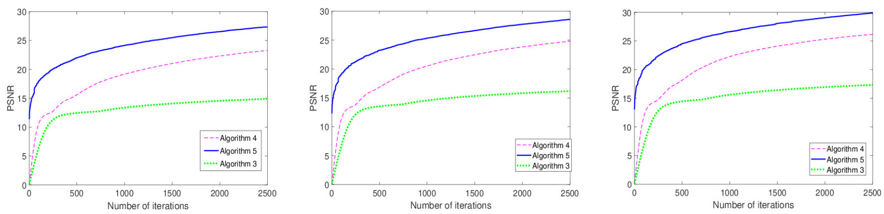

(a) PSNR (Red) (b) PSNR (Green) (c) PSNR (Blue)

Figure 13: Graphs of PSNR for red, green and blue for Algorithms 3, 4 and 5 of Temple image with motion length 45.

From Figures 11-13, it is observed that the PSNR of red, green and blue of Algorithm 5 is higher than Algorithms 3 and 4 in comparison. It shows the applicability and efficiency the proposed method for solving the image deblurring problem which is the application of the SFP.

7. Conclusions

In this work, we proposed new and efficient algorithms for the split feasibility problem. We show that the sequence generated by the proposed method converges weakly to a solution of the SFP. The numerical experiments reveal that our algorithms outperform algorithms defined by Zhao et al. [37] and Dong et al. [12].

Acknowledgments

This project is funded by National Research Council of Thailand (NRCT) under grant no. N41A640094. The authors wish to thank University of Phayao and Thailand Science Research and Innovation grant no. FF65-UoE001.

References

[1] A.S. Antipin, On a method for convex programs using a symmetrical modification of the Lagrange function, Ekon. Mat. Metody 12, (1976)1164-1173.
[2] H.H. Bauschke, P.L. Combettes, A weak-to-strong convergence principle for Fejér-monotone methods in Hilbert spaces. Math. Oper. Res. 26, (2001)248-264.
[3] H.H. Bauschke, P.L. Combettes, Convex Analysis and Monotone Operator Theory in Hilbert Spaces, Springer, London (2011).
[4] C. Byrne, Iterative oblique projection onto convex sets and the split feasibility problem, Inverse Probl. 18, (2002)441-453.
[5] C. Byrne, A unified treatment of some iterative algorithms in signal processing and image reconstruction, Inverse Probl. 20, (2004)103-120.
[6] Y. Censor, A. Gibali, S. Reich, Algorithms for the split variational inequality problem, Numer Algor. 59(2),(2012)301-323.
[7] Y. Censor, T. Bortfeld, B. Martin, A. Trofimov, A unified approach for inversion problems in intensity-modulated radiation therapy, Phys. Med. Biol. 51, (2003)2353-2365.
[8] Y. Censor, T. Bortfeld, B. Martin, A. Trofimov, The split feasibility model leading to a unified approach for inversion problems in intensity-modulated radiation therapy, Technical Report 20 April: Department of Mathematics, University of Haifa, Israel, 2005.
[9] Y. Censor, T. Elfving, A multiprojection algorithms using Bregman projection in a product space, Numer. Algor. 8, (1994)221-239.
[10] Y. Censor, T. Elfving, N. Kopf, T. Bortfeld, The multiple-sets split feasibility problem and its applications for inverse problem, Inverse Prob. 21, (2005)2071-2084.
[11] Y. Censor, M. Jiang, G. Wang, Iterative algorithms for the multiple-sets split feasibility problem. In editors: Biomedical mathematics: promising directions in imaging therapy planning and inverse problems. Madison (WI): Medical Physics Publishing., (2010)243-279.
[12] Q.L. Dong, Y.C. Tang, Y.J. Cho, T.M. Rassias, Optimal choice of the step length of the projection and contraction methods for solving the split feasibility problem, J. Glob.Optim., 71(2), (2018) 341-360.
[13] B. Eicke, Iteration methods for convexly constrained ill-posed problems in Hilbert spaces, Numer. Funct. Anal. Optim. 13, (1992)413-29.
[14] M. Fukushima, A relaxed projection method for variational inequalities, Math. Program. 35, (1986)58-70.
[15] S. Kesornprom, N. Pholasa, P. Cholamjiak, On the convergence analysis of the gradient-CQ algorithms for the split feasibility problem, Numer. Alg., (2019)1-21
[16] S. Kesornprom, P. Cholamjiak, Proximal type algorithms involving linesearch and inertial technique for split variational inclusion problem in hilbert spaces with applications, Optim. 68(12), (2019)2369-2395
[17] G.M. Korpelevich, The extragradient method for finding saddle points and other problems, Ekon. Mate. Metody 12, (1976)747-756.
[18] A. Gibali, A new split inverse problem and application to least intensity feasible solutions, Pure Appl. Funct. Anal. 2, (2017)243-258.
[19] A. Gibali, L.W. Liu, Y.C. Tang, Note on the modified relaxation CQ algorithm for the split feasibility problem, Optim. Lett. 12, (2017)1-14.
[20] A. Gibali, K.H. Küfer, P. Süss, Successive linear programing approach for solving the nonlinear split feasibility problem, Journal of Nonlinear and Convex Analysis, 15, (2014)345-353.
[21] Z. Opial, Weak convergence of the sequence of successive approximations for nonexpansive mappings, Bull Am Math Soc. 73(4), (1967)591-597.
[22] S. Penfold, R. Zalas, M. Casiraghi, M. Brooke, Y. Censor, R. Schulte, Sparsity constrained split feasibility for dose-volume constraints in inverse planning of intensity-modulated photon or proton therapy, Physics in Medicine and Biology 62, (2017)3599-3618.
[23] L. Landweber, An iterative formula for Fredholm integral equations of the first kind, Am. J.Math. 73(3), (1951)615-624.
[24] Z. Li, D. Han, W. Zhang, A self-adaptive projection-type method for nonlinear multiple-sets split feasibility problem, Inverse Problems in Science and Engineering iFirst,(2012) 1-16.

[25] G. López, V. Martín-Márquez, F.H. Wang, H.K. Xu, Solving the split feasibility problem without prior knowledge of matrix norms, Inverse Prob. 2012. doi:10.1088/0266-5611/28/8/085004.
[26] G. López, V. Martín-Márquez, H.K. Xu, Perturbation techniques for nonexpansive mappings with applications, Nonlinear Anal. RealWord Appl. , 10, (2009)2369-2383.
[27] B. Qu, N. Xiu, A note on the CQ algorithm for the split feasibility problem, Inverse Prob. 21, (2005)1655-1665.
[28] B. Qu, N. Xiu, A new halfspace-relaxation projection method for the split feasibility problem, Linear Algebr. Appl. 428, (2008)1218-1229.
[29] R.T. Rockafellar, Monotone operators and the proximal point algorithm, SIAM J. Control Optim. 14, (1976)877-898.
[30] S. Suantai, S. Kesornprom, P. Cholamjiak, A new hybrid CQ algorithm for the split feasibility problem in Hilbert spaces and Its applications to compressed Sensing. Math. 7(9), (2019)789.
[31] S. Suantai, S. Kesornprom, P. Cholamjiak, Modified Proximal Algorithms for Finding Solutions of the Split Variational Inclusions, Math. 7(8), (2019)708.
[32] P. Tseng, A modified forward-backward splitting method for maximal monotone mappings, SIAM J. Control Optim. 38, (2000)431-446.
[33] R. Tibshirani, Regression shrinkage and selection via the lasso, J. R. Stat. Soc. Ser. B. Stat. Methodol. 58, (1996)267-288.
[34] H.K. Xu, Iterative methods for the split feasibility problem in infinite-dimensional Hilbert spaces, Inverse Prob. 26, (2010)105018.
[35] Q. Yang, The relaxed CQ algorithm for solving the split feasibility problem, Inverse Prob, 20, (2004)1261-1266.
[36] W. Zhang, D. Han, Z. Li, A self-adaptive projectionmethod for solving themultiple-sets split feasibility problem, Inverse Probl. 25, (2009)115001.
[37] J. Zhao, Y. Zhang, Q. Yang, Modified projection methods for the split feasibility problem and the multiple-sets split feasibility problem, Appl. Math. Comput. 219(4), (2012)1644-1653.
[38] J. Zhao, Q. Yang, Self-adaptive projectionmethods for the multiple-sets split feasibility problem, Inverse Probl. 27, (2011)035009.